SAND2020-1666C

Evaluation of XHVRB for Capturing Transition to Detonation as Measured by Embedded Gauges

Leah W. Tuttle[1, a)], Jeff W. LaJeunesse[1], Robert G. Schmitt[1], and Eric N. Harstad[1]

[1]*Sandia National Laboratories, Albuquerque, NM 87185, USA*

[a)]*Corresponding author: lworrel@sandia.gov*

Abstract. The Extended History Variable Reactive Burn model (XHVRB), as proposed by Starkenburg, uses shock capturing rather than current pressure for calculating the pseudo-entropy that is used to model the reaction rate of detonating explosives. In addition to its extended capabilities for modeling explosive desensitization in multi-shock environments, XHVRB's shock capturing offers potential improvement for single shock modeling over the historically used workhorse model HVRB in CTH, an Eulerian shock physics code developed at Sandia National Labs. The detailed transition to detonation of PBX9501, as revealed by embedded gauge data, is compared to models with both HVRB and XHVRB. Improvements to the comparison of model to test data are shown with XHVRB, though not all of the details of the transition are captured by these single-rate models.

INTRODUCTION

Historically, pressure-based reactive flow models were fit using Pop plot data [1], which gave information about the run distance and time to detonation as a function of the input pressure. In the last two decades, new experimental techniques have been developed that reveal more detailed information about the transition to detonation. The most revealing of these is the embedded gauge data that measures particle velocity at varying depths in the explosive [2]. This data shows the build up to transition and provides a more rigorous test for reactive flow models than Pop plot data. Newer models, like CREST [3], are built around this new understanding and use the data in the complex process of fitting the models for different explosives, but other models can use this data as a way to test their accuracy and usability. In this paper, HVRB [1] and XHVRB [4,5] are run in CTH [6] to compare simulation with embedded gauge data on PBX 9501, an HMX-based explosive.

MODEL DESCRIPTION

HVRB has been a heavily used model in CTH for shock-to-detonation problems due to its simplicity and usability. HVRB is relatively easy to fit, given Pop plot data, and it is very good at modeling the run distance accurately, but it is a single rate model that depends on local pressure only [1]. This model cannot capture desensitization effects, and it has to be refit to Pop plot data at the relevant temperature or initial density in order to model the explosive behavior correctly under such conditions. XHVRB is a newer model, based on HVRB, that captures the shock pressure and calculates the reaction rate based on the pseudo entropy [4]. XHVRB has shown promise for capturing desensitization in multi-shock scenarios in 1D [4,7] and in multidimensional scenarios [8].

Both HVRB and XHVRB use the Mie-Gruneisen equation of state (EOS) to represent the unreacted explosive, which is fit based on Hugoniot data. Additionally, both models use the Sesame EOS for the reacted products expansion, calculated with thermochemical equilibrium codes like Tiger [9] and compared to cylinder expansion data. The reaction rate parameters of the models are fit to Pop plot data, and additional data that reveals information about the explosive's sensitivity to desensitization is needed for XHVRB if it is going to be used in multi-shock scenarios. The details of the transition to detonation have not been considered in the fitting of these models until now.

Sandia National Laboratories is a multimission laboratory managed and operated by National Technology & Engineering Solutions of Sandia, LLC, a wholly owned subsidiary of Honeywell International Inc., for the U.S. Department of Energy's National Nuclear Security Administration under contract DE-NA0003525.

METHODOLOGY

Tests done by Gustavsen et al. [2] looked at the explosive PBX9501 at three different densities and at different ages. This study included 20 tests done in a gas gun, all of which used the embedded gauge package to get data on the particle velocity during the transition to detonation (though a few were unsuccessful). For this study, three tests were selected from the Gustavsen study, all done on samples at the highest density tested (1.837 g/cm^3) and all using a Vistal impactor [2]. The three tests chosen were 1144, 1150, and 1165, which had different impact velocities giving three different input conditions. These tests were chosen for their consistency in set up, and because they revealed three different build-ups showing features of interest for comparison with simulated results.

Simulations were done with a mesh resolution of 0.01 mm in a 1D flat mesh. The Mie-Gruneisen EOS was used for Vistal, and for the Lexan impactor holder. The explosive sample was approximately an inch in thickness. Tracers were placed at the test gauge locations. The set-up is depicted in Fig. 1. Both HVRB and XHVRB models used the default Mie-Gruneisen EOS in the CTH library for the unreacted PBX9501 explosive. Both also use the default Sesame table from the CTH library. The Pop plot produced by the default rate parameters in the CTH library for PBX9501 was compared to the Pop plot data reported by Gustavsen et al. A small adjustment was made to the reaction rate parameters such that the model matched the Pop plot for the 1.837 g/cm^3 density very closely. XHVRB was fit from scratch to the same Pop plot, though it used the HVRB reaction rate parameters as a starting point. This fit was done to get initial results.

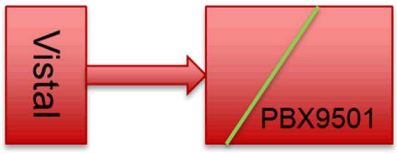

FIGURE 1. Test set up showing Vistal impactor and PBX9501 sample; the green line depicting gauges placed along a wedge.

RESULTS

Results showing the comparisons of XHVRB and HVRB simulated results with experiment for all three tests selected are shown in Fig. 2. A qualitative assessment of the comparisons shows excellent agreement between XHVRB and the test data from shot 1144, with similar curvature evident in the velocity profile comparisons. HVRB shows a different qualitative shape in the velocity curves, with a concave “up” shape and a sharper rise to the steady-state detonation. Both models show good agreement in the arrival time at each gauge and in the initial shock state at the early gauges, with XHVRB showing good agreement at almost all the gauges. Comparisons of tests 1150 and 1165 were not as good for either model. HVRB shows marked differences in the shape of the velocity traces for these tests, both of which had a lower input condition than 1144. XHVRB has some similarity to the measured data in its shape, showing the hill-shaped growth but not the linear initial rise at each gauge. The same model shows good agreement in the arrival time and magnitude of velocity in 1150, but shows good agreement only in arrival time in 1165.

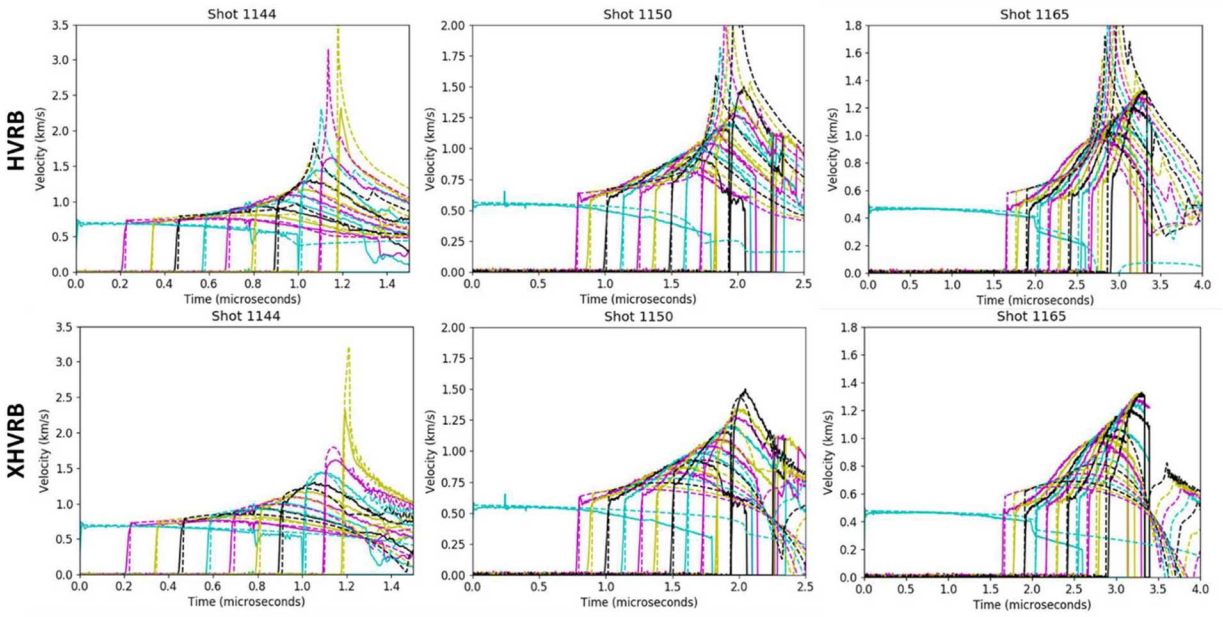

FIGURE 2. Comparison of embedded gauge data to simulation results for HVRB (top row) and XHVRB (bottom row) for shots 1144 (left), 1150 (center), and 1165 (right). Experimental gauge data is shown as solid lines, and simulation data as dashed lines.

In trying to quantify the similarities and differences that were apparent to the eye, James and Lambourn [10] suggested some quantitative metrics. In their study, they recorded (for both test and simulation) the arrival time at each gauge (tshk), the shock magnitude (the magnitude of particle velocity at time of arrival) at each gauge (ushk), the peak particle velocity reached at each gauge (upk), and the time at which the peak was seen (tpk). These four quantities were plotted in several different ways. One of these, which is analogous to the Pop plot, is the plot of the first shock arrival magnitude versus the time shift, or the time between shock arrival and peak particle velocity, in log-log space. In the James paper, the same data from the Gustavsen study was plotted in this way and showed a remarkable collapsing onto a single line, suggesting that, like the Pop plot, the input shock condition is the driving force for the reaction rate. The data for all 20 tests fell along a single line in this plot. This agrees with current thinking that a reaction rate dependent on the shock state is a significant improvement over local pressure for modeling reactive flow processes well. The data from the three shots discussed here are plotted in that space (Fig. 3), along with the data from the CTH simulations using the HVRB and XHVRB models. As expected, the test data lines up nicely. In the XHVRB case, the simulation data follows that same line, though each point does not fall directly on each corresponding test point. This may suggest that, though XHVRB does not capture all four of the metrics exactly right, the modeled explosive is behaving in a similar way to the test data. HVRB shows a different trend, though it is not far off the test data.

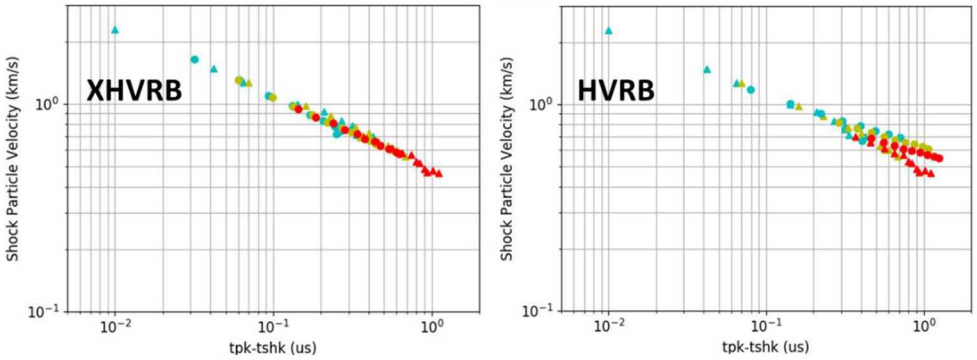

FIGURE 3. Log-log plot of shock particle velocity versus the time difference between shock arrival and peak shock velocity for test 1144 (blue triangles), 1150 (yellow triangles) and 1165 (red triangles), plotted with the results from simulations of shot 1144 (blue circles), 1150 (yellow circles) and 1165 (red circles). Results for XHVRB are on the left, and for HVRB are on the right.

Of the four metrics identified in the James paper, only three are represented by the above plot. Another plot takes into consideration the 4th quantity, the peak velocity, by plotting the difference in initial shock particle velocity (ushk) and peak particle velocity (upk), normalized by the initial input velocity (uo), versus the time of arrival of the initial shock. This plot (Fig. 4) shows significant difference for both XHVRB and HVRB. XHVRB seems to be trending farther away from the data as the input pressure drops (so 1144 is a closer match than 1165, which is also visually apparent).

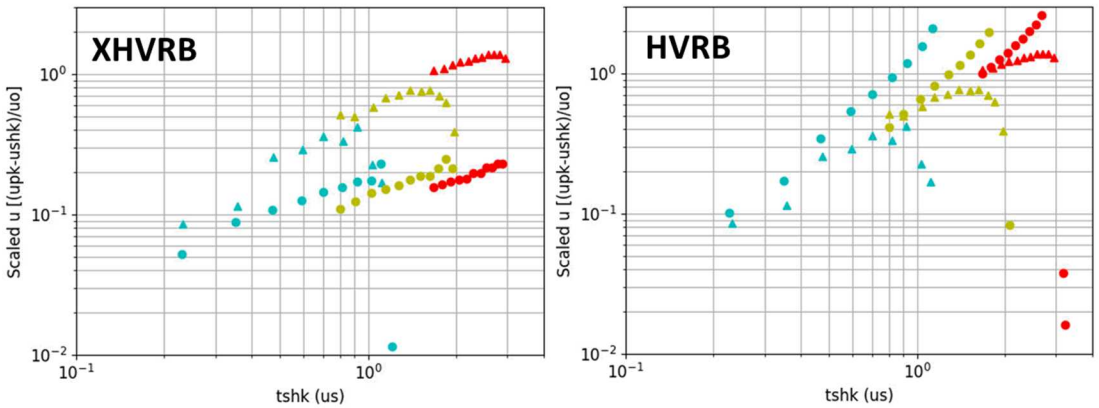

FIGURE 4. Log-log plot the scaled peak velocity, which is the peak velocity minus the shock velocity divided by the initial shock input velocity, for test 1144 (blue triangles), 1150 (yellow triangles) and 1165 (red triangles), plotted with the results from simulations of shot 1144 (blue circles), 1150 (yellow circles) and 1165 (red circles). Results for XHVRB are on the left, and for HVRB are on the right.

With these new plots in hand, a sensitivity study was done in which the reaction rate parameters PR, ZR, and MR were varied within ranges, and the simulation results were plotted on both Pop plots and these new log-log plots. Out of the five parameters of HVRB, these three were chosen because they have the greatest effect on the model behavior. In the case of the Pop plots, best fit lines were drawn through both simulation and test data, and these lines were compared. The metrics taken from the embedded gauge data were compared point-to-point. An error was calculated for each of 4 plots (Pop plot based on time, Pop plot based on run distance, and each of the two log-log plots described above), and the error of the four plots were summed to give an overall error. In this way, the best fits were chosen. The results shown in Figs. 2-4 represent the best fit achieved from this quantitative approach. The fits to the Pop plot in both time and run distance space are shown in Fig. 5.

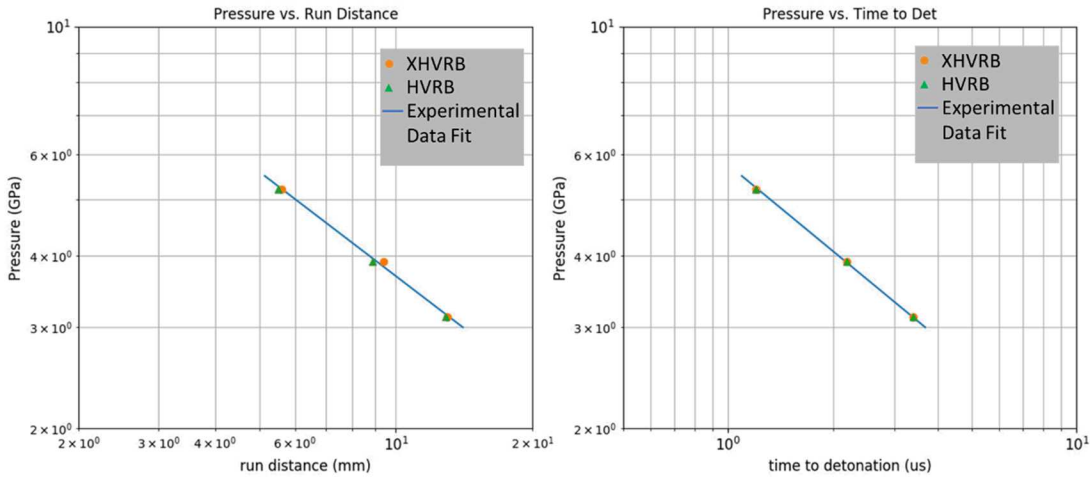

FIGRUE 5. Pop plots for pressure versus run distance (left) and time to detonation (right) for both XHVRB and HVRB.

One further qualitative comparison is offered here to highlight some of the similarities and differences each of the reactive models has in comparison to the embedded gauge data. Fig. 6 shows two gauge comparisons from tests 1144 (left) and 1165 (right). The time histories for gauge #2 from both test 1144 and the simulation done with XHVRB look remarkably similar until late in time. HVRB is also similar but shows a growth around 1 μs that is different from the test data and the results of XHVRB. Comparison of the results from gauge #8 again shows good agreement between test and XHVRB, but HVRB is clearly different, growing from a lower initial shock particle velocity and showing a much sharper, and higher, peak. Comparisons from 1165 highlight some of the differences between the test data and both models, with XHVRB overpredicting the initial particle velocity magnitude and showing less growth overall than is seen in the test data. HVRB continues to show the sharp peak at each simulated gauge that is not evident in the test data. The gauges from test 1165 seem to show two different shapes in the growth, which suggests that early reaction is happening at a different rate than late reaction. The concave-up shape of HVRB is not similar to the test data. XHVRB captures the hill-shaped growth, but not the initial growth shape. A single-rate model cannot capture both of these shapes.

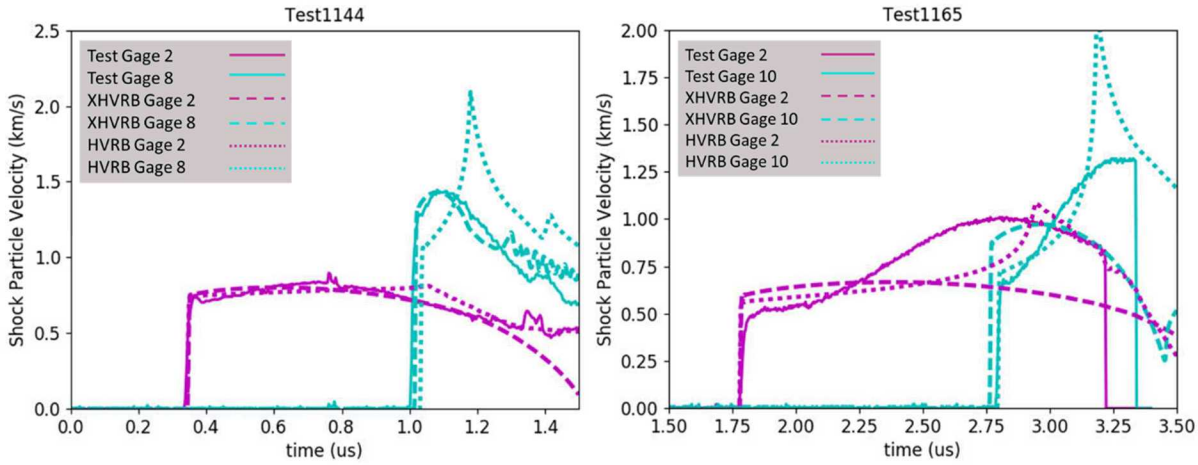

FIGURE 6. Selected gauge comparisons between test data (solid lines), XHVRB simulation results (dashed lines) and HVRB simulation results (dot-dashed lines).

DISCUSSION

Simulated results from the reactive burn models HVRB and XHVRB have been compared to data from embedded gauge tests to examine their ability to capture the details of the transition to detonation. While XHVRB shows more similarity to the embedded gauge data, what may be multi-rate effects will not be captured by either of these models. The new metrics that have been identified by James and Lambourn are useful for evaluating current reactive flow models against this new and more detailed data. Using these metrics, a quantitative evaluation of the model fit to the embedded gauge data was performed, and a "best fit" case shows very good agreement with three of the four metrics along with the Pop plot, but there are differences in the measured and simulated peak particle velocities. Overall, XHVRB shows an improvement over HVRB for capturing the details of shock-to-detonation transition as revealed by embedded gauge data, but neither model can capture all of the details, particularly when multi-rate behavior is observed.

ACKNOWLEDGMENTS

The authors would like to thank Dave Kittell, Mike Hobbs, Bill Erikson, Kevin Ruggirello, Paul Specht, Ryan Marinis, and Nick Kerschen for valuable input and peer review. Sandia National Laboratories is a multimission laboratory managed and operated by National Technology and Engineering Solutions of Sandia, LLC, a wholly owned subsidiary of Honeywell International, Inc., for the U.S. Department of Energy's National Nuclear Security Administration under contract DE-NA0003525.

REFERENCES

1. Kerley, G. I., Sandia National Labs internal report, SAND92-0553, 1992
2. R. L. Gustavsen, S. A. Sheffield, R. R. Alcon, and L. G. Hill, *Proceedings of the 12th Int. Detonation Symposium*, July 2002, p. 530
3. C. A. Handley, *Proceedings of the 13th Int. Detonation Symposium*, Norfolk, VA, 2006, p. 864
4. J. Starkenberg, *Proceedings of the 15th Int. Detonation Symposium*, San Francisco, CA, 2014, p. 908
5. Tuttle, L., et al., *AIP Conf. Proc.*, **1979**, 100044 (2018), DOI:10.1063/1.5044916
6. McGlaun, J. M., et. al, Int. Journal of Impact Eng., Vol. 10, p. 351
7. L. W. Tuttle, R. G. Schmitt, D. E. Kittell, E. N. Harstad, *Proceedings of the 16th Int. Detonation Symposium*, Cambridge, MD, July 2018, p. 1173
8. L. W. Tuttle, R. T. Marinis, R. G. Schmitt, D. E. Kittell, E. N. Harstad, *Proceedings of the 16th Int. Detonation Symposium*, Cambridge, MD, July 2018, p. 618
9. M. L. Hobbs, R. G. Schmitt, H. K. Moffat, Z. Lawless, *Proceedings of the 16th Int. Detonation Symposium*, Cambridge, MD, July 2018, p.651
10. James, H. R., et al., J. Appl. Phys. **100**, 084906 (2006), DOI:10.1063/1.2354416